Dependence of Single- and Multi-Helicity States on Θ and the Hartmann number in the Force-free Visco-resistive MHD Model

D. D. Schnack
Department of Physics
University of Wisconsin - Madison
Madison, WI 53706

November 11, 2013

Abstract

Converged computations with the DEBS code indicate that, within the force-free resistive MHD model in a doubly periodic cylinder with perfectly conducting boundary conditions, the appearance of single-helicity or multi-helicity states is determined primarily by the Hartmann number, and is relatively independent of the pinch parameter or the degree of field reversal.

1 Similarity Scaling in Visco-resistive MHD

Many aspects of RFP dynamics are well described with the force-free visco-resistive MHD model[1]. In MKS units, the equations of this model are

$$\frac{d\mathbf{V}}{dt} = \frac{1}{\rho}\mathbf{J}\times\mathbf{B} + \nu\nabla^2\mathbf{V} \ , \tag{1}$$

and

$$\frac{\partial\mathbf{B}}{\partial t} = \nabla\times(\mathbf{V}\times\mathbf{B}) + \frac{\eta}{\mu_0}\nabla^2\mathbf{B} \ , \tag{2}$$

where $\nu = \mu/\rho$ is the kinematic viscosity, η is the resistivity, $\mu_0\mathbf{J} = \nabla\times\mathbf{B}$ and $d/dt \equiv \partial/\partial t + \mathbf{V}\cdot\nabla\mathbf{V}$. These equations admit non-solenoidal flows ($\nabla\cdot\mathbf{V} \neq 0$), so that the implied stress tensor $\mathbf{\Pi} = \nu\nabla\mathbf{V}$ is neither symmetric nor invariant

under rigid rotations and is therefore unphysical. Nonetheless, the model is widely used in computational modeling of RFP plasmas[1, 2, 3]. The mass density ρ is assumed to be constant and spatially uniform. These equations are usually solved in doubly periodic cylindrical geometry with boundary conditions suitable for a perfectly conducting, impermeable wall. That is the case here.

Equations (1-2) admit three characteristic time scales: the Alfvén transit time $\tau_A = a/V_A$, the resistive diffusion time $\tau_R = \mu_0 a^2/\eta$, and the viscous diffusion time $\tau_\nu = a^2/\nu$, where $V_A = B_0/\sqrt{\mu_0 \rho}$ is the Alfvén velocity, B_0 is a characteristic value of the magnetic field, and a is a characteristic length scale. Several non-dimensional parameters can be formed from these time scales: the Lundquist number, $S = \tau_R/\tau_A$; the viscous Lundquist number $S_\nu = \tau_\nu/\tau_A$; and, the magnetic Prandtl number $P_M = \tau_R/\tau_\nu$. Generally both S and S_ν are $>> 1$. If we measure time in units of $\tau_0 = \tau_A$ and the velocity in units of $V_0 = V_A$, then Equations (1) and (2) can be written in non-dimensional form as

$$\frac{d\mathbf{V}}{dt} = \Theta_0 \mathbf{J} \times \mathbf{B} + \frac{1}{S_\nu} \nabla^2 \mathbf{V} \ , \tag{3}$$

and

$$\frac{\partial \mathbf{B}}{\partial t} = \nabla \times (\mathbf{V} \times \mathbf{B}) + \frac{1}{S} \nabla^2 \mathbf{B} \ , \tag{4}$$

where $\Theta_0 = B_\theta(a)/B_0$ is the Pinch parameter (this assumes a cylindrical plasma of radius a; Θ_0 is a measure of the amount of current being driven in the plasma relative to the amount of axial (z) magnetic flux). These equations imply that the state and dynamics of the discharge are determined by the three non-dimensional parameters S, S_ν, and Θ.

Since the dynamics depend on both resistive (τ_R) and viscous (τ_ν) dissipation, we are motivated[4, 5] to define a hybrid time scale $\tau_0 = a/V_0 = \tau_R^\alpha \tau_\nu^{1-\alpha}$, where V_0 is the normalization of the velocity. Substituting into Equations (1) and (2), and dividing the momentum equation by $(\tau_0/\tau_A)^2$, we find that the non-dimensional diffusion coefficients of the two equations become equal when $\alpha = 1/2$. Then choosing $\tau_0 = \sqrt{\tau_R/\tau_\nu}\tau_A$ and $V_0 = \sqrt{\tau_\nu/\tau_R} V_A$, the non-dimensional visco-resistive equations become

$$\frac{1}{P_M}\frac{d\mathbf{V}}{dt} = \Theta_0 \mathbf{J} \times \mathbf{B} + \frac{1}{H} \nabla^2 \mathbf{V} \ , \tag{5}$$

and

$$\frac{\partial \mathbf{B}}{\partial t} = \nabla \times (\mathbf{V} \times \mathbf{B}) + \frac{1}{H} \nabla^2 \mathbf{B} \ , \tag{6}$$

where $H \equiv \sqrt{\tau_R \tau_\nu}/\tau_A = a V_A/\sqrt{\nu(\eta/\mu_0)}$ is the Hartmann number. It is related to S and P_M by $S^2 = P_M H^2$.

The dynamical behavior of the system is still determined by three non-dimensional parameters, in this case H, P_M, and Θ_0. However, consider the linearized equations in a cylinder with no mean flow (so that the contribution of $\mathbf{V}\cdot\nabla\mathbf{V}$ can be ignored). With time dependence $e^{-i\omega t}$, these are

$$-\frac{1}{P_M}i\omega\mathbf{V}_1 = \Theta_0\left(\mathbf{J}_1\times\mathbf{B}_0 + \mathbf{J}_0\times\mathbf{B}_1\right) + \frac{1}{H}\nabla^2\mathbf{V}_1 \ , \tag{7}$$

and

$$-i\omega\mathbf{B}_1 = \nabla\times\left(\mathbf{V}_1\times\mathbf{B}_0\right) + \frac{1}{H}\nabla^2\mathbf{B}_1 \ . \tag{8}$$

The marginally stable state is found by setting $\omega = 0$, so that this state depends only on the *two* non-dimensional parameters Θ_0 and H; the marginal linear stability properties of a cylindrical pinch depend only on these two parameters. For a given Θ_0 (system drive), the marginal stability point depends on the dissipation only through H, and not on S (resistivity) or S_ν (viscosity) independently. *Both dissipation mechanisms contribute equally to the stability properties of the system.* This result was first shown by Montgomery[4]. As stated in Ref. [4], "It has had the status of occasional folk wisdom that viscosity could be neglected in stability analysis while retaining resistivity — a statement which the foregoing conclusions suggest is untrue."

Further, consider non-linear states in which inertia is unimportant (i.e., $d\mathbf{V}/dt \sim 0$). The properties of these states also depend only on Θ_0 and H. This was first pointed out by Cappello and Escande[5] in the context of RFP quasi-steady states. For a pure steady state ($\partial\mathbf{V}/\partial t = 0$), this implies that $|\mathbf{V}\cdot\nabla\mathbf{V}| << (P_M/H)|\nabla^2\mathbf{V}|$, which may or may not be true in any particular instant of time. However, if we consider a time average steady state (with fluctuations about some mean, say), then $< d\mathbf{V}/dt >=< \partial\mathbf{B}/\partial t >= 0$, and the time average properties of this state, such as its harmonic content or amount of field reversal, must depend only on Θ_0 and H, and not on either resistivity or viscosity individually. The importance of viscosity in determining the quasi-steady state properties of RFPs was first pointed out by Cappello and Paccagnella[6].

Cappello and Escande[5] considered only the dependence on the Hartmann number. They performed a series of numerical simulations[3] with varying H at a fixed value of $\Theta_0 = 1.9$ and aspect ratio $R/a = 4$. They varied H by keeping S constant and varying P_M. Scans in H were performed for two different values of S: $S = 3.3\times10^3$, $S = 3\times10^4$. For each case they measured the time average energy in the $m = 0$ perturbations, and used this as a means of distinguishing single helicity (SH) and multi-helicity (MH) states. They reasoned that the $m = 0$ modes are driven by the non-linear interaction of the $m = 1$ dynamo modes. For a single helicity state (dominated by a single $m = 1$ mode) there would be no such interactions and the $m = 0$ energy would be small, while for a multi-helicity state

(with several interacting $m = 1$ dynamo modes) the $m = 0$ energy would be driven to a significantly larger value. Their computations showed that the $m = 0$ energy had a significant increase when H was raised above $\sim 2000 - 3000$, independent of S. Their results (their Figure 2) are reproduced in Figure 1. They interpreted this as a transition from single helicity to multi-helicity states when H exceeded a few thousand. They did not investigate the dependence on Θ_0, or determine the dependence of the marginal stability point on H.

2 DEBS Computations

The MH and SH states are differentiated by the number of helical $m = 1$ modes present. A convenient diagnostic for this purpose is the parameter[8]

$$N_s = \frac{1}{\sum_n \left[\frac{W_{1,n}}{\sum_{n'} W_{1,n'}}\right]^2} , \tag{9}$$

where $W_{1,n}$ is the energy in the helical mode with poloidal mode number $m = 1$ and axial mode number n. Equation (9) has the property that $N_s = 1$ when a single mode $m = 1$ is present. These states are SH; all others are classified as MH. This is also the diagnostic used to analyze experiments[9, 10].

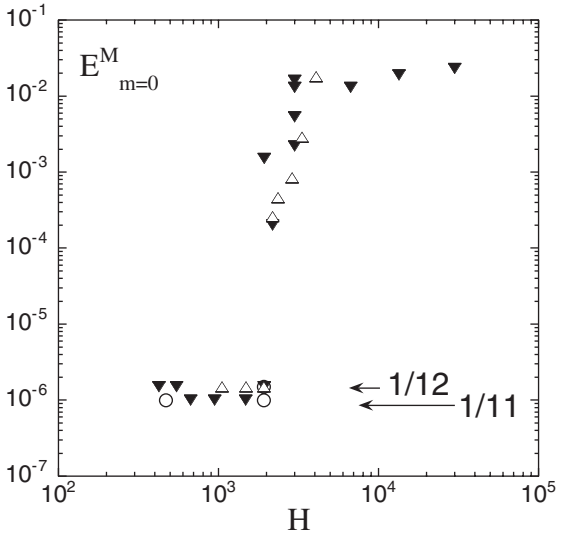

Figure 1: The magnetic energy in $m = 0$ modes as a function of Hartmann number for $\Theta = 1.9$, $R/a = 4$, and two different values of S: $S = 3.3 \times 10^3$ (open triangles) and $S = 3 \times 10^4$ (black triangles). This is a reproduction of Figure 2 of Ref. [5].

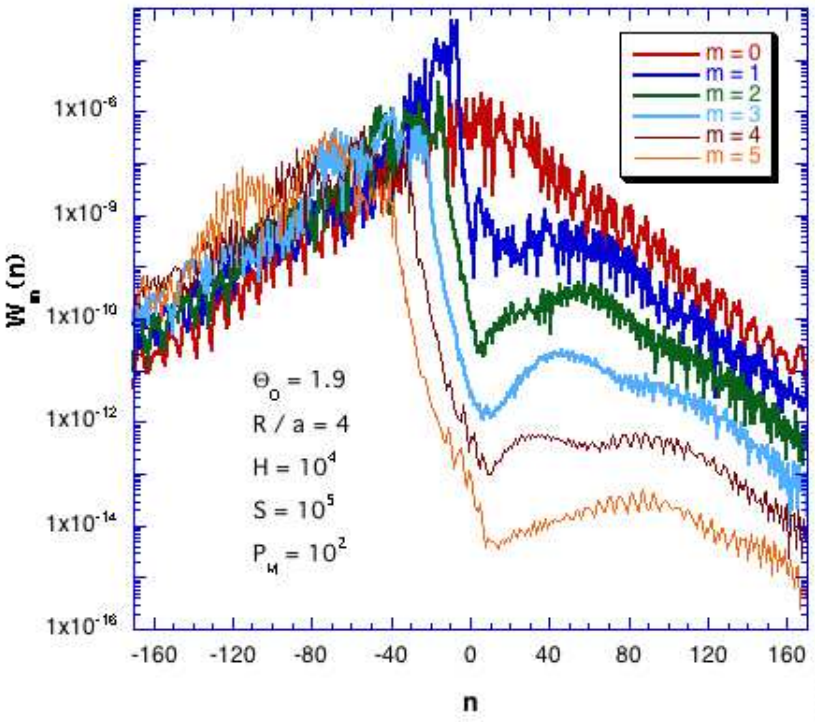

Figure 2: The axial mode spectrum for the case $\Theta_0 = 1.9$, $R/a = 4$, $H = 10^4$, $S = 10^5$ and $P_M = 10^2$.

We have used the DEBS code[2] to solve the force-free visco-resistive MHD equations as an initial value problem in a doubly periodic cylinder. We have used boundary conditions suitable to a perfectly conducting wall at $r = a$: $B_r(a) = V_r(a) = 0$. We then determine the value of N_s as a function of Hartmann number using the same parameters as Ref. [5] ($\Theta_0 = 1.9$, $R/a = 4$). (For all results presented here, the plotted value of N_s is the *time average* of the instantaneous value of N_s. Also, in DEBS, B_0 is taken to be the magnetic field at $r = 0$, and the pinch parameter is defined as $\Theta_0 = B_\theta(a)/ < B >$, where $< B >$ is the *average* of B_z and is proportional to the total axial flux.) In addition to $S = 3.3 \times 10^3$ and $S = 3 \times 10^4$ considered in Ref. [5], we have also included $S = 10^5$. We have used a resolution of $N_r = 50$ radial points, poloidal mode numbers $0 \leq m \leq 5$, and axial mode numbers $-170 \leq n \leq 170$. We have found that the radial resolution is sufficient, and the axial mode (n) spectrum is well resolved for all m. An example of the spectrum for $\Theta_0 = 1.9$, $R/a = 4$, $H = 10^4$, $S = 10^5$ and $P_M = 10^2$ is shown in Figure 2. The amplitude of several $n = 1$ modes near $n = -10$ indicates multi-helicity (MH). Single helicity (SH) cases are dominated by a single $(m = 1, n)$ mode.

The results can also depend on the size of the time step Δt. We have assured that the results presented below are independent of Δt.

In Figure 3 we plot N_s as a function of H for these parameters. There is a transition from SH ($N_s = 1$) to MH ($N_s > 1$) at $H \sim 2000 - 3000$ independent of S, in substantial agreement with Ref. [5]. We also find that marginal stability occurs at $H \sim 200$, independent of the individual values of S and P_M, confirming the predictions of Ref. [4].

Since both marginal stability and the properties of time average steady states depend only on the parameters Θ_0 and H, we have repeated these calculations for several different values of Θ_0 for $R/a = 4$. The results are shown in Figure 4, where we plot N_s vs. Θ_0 for different values of H and S. All cases with $H = 10^3$ are single helicity ($N_s = 1$), as is the case $H = 10^4$ and $S = 3.3 \times 10^3$. While there is clearly a trend toward fewer $m = 1$ modes with decreasing Θ_0, the presence of single helicity ($N_s = 1$) is most strongly influenced by H. The marginal stability point ($N_s = 0$) is approximately constant for a given value of H, independent of S, consistent with Ref. [4], although the results are not as clear as in Figure 3.

In the RFP, the reversal parameter $F = B_z(a)/B_0$ is a function of the pinch parameter Θ_0[7]; reversal occurs when $F < 0$. In visco-resistive MHD computations we specify $B_\theta(a)$ through the values of Θ_0 and B_0; the latter is given by the initial value of the axial magnetic flux, which is conserved. The value of F is then determined by the dynamics; it is output. Therefore, from our data we can determine F as a function of Θ_0 for different values of H and S. The results are shown in Figure 5. For these parameters, reversal occurs in the range $1.45 < \Theta_0 < 1.7$.

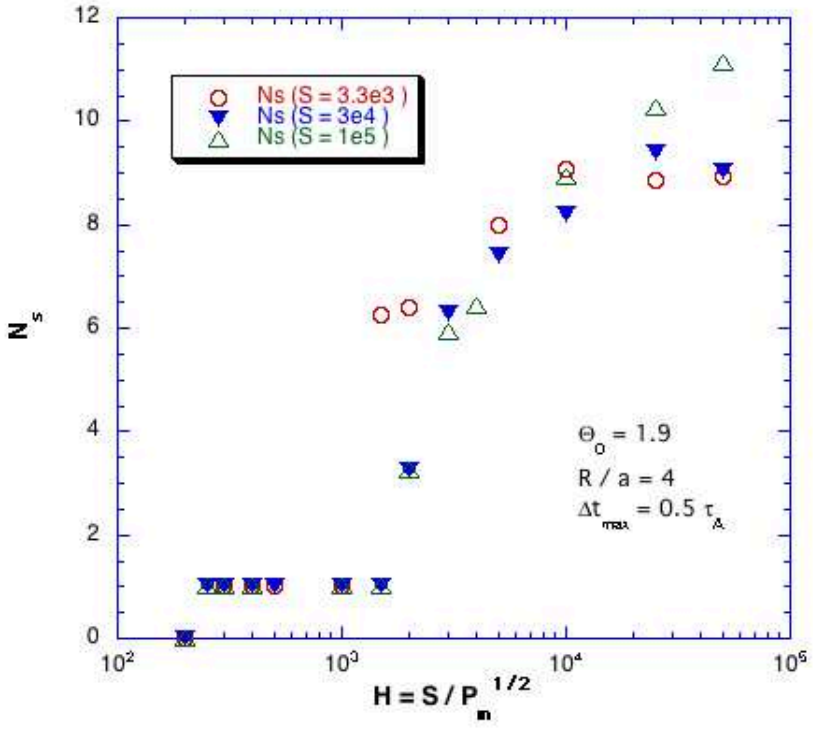

Figure 3: N_s, the number of $m = 1$ mode present in the time asymptotic state, as a function of the Hartmann number for $\Theta_0 = 1.9$, $R/a = 4$, and three values of S: $S = 3.3 \times 10^3$, $S = 3 \times 10^4$, and $S = 10^5$. For these parameters, there is a transition from single helicity (SH), $N_s = 1$, to multi-helicity (MH), $N_s > 1$, at $H \sim 2000 - 3000$ independent of S, in substantial agreement with Ref. [5]. The marginal stability point occurs at $H \sim 200$, independent of S, confirming the results of Ref. [4].

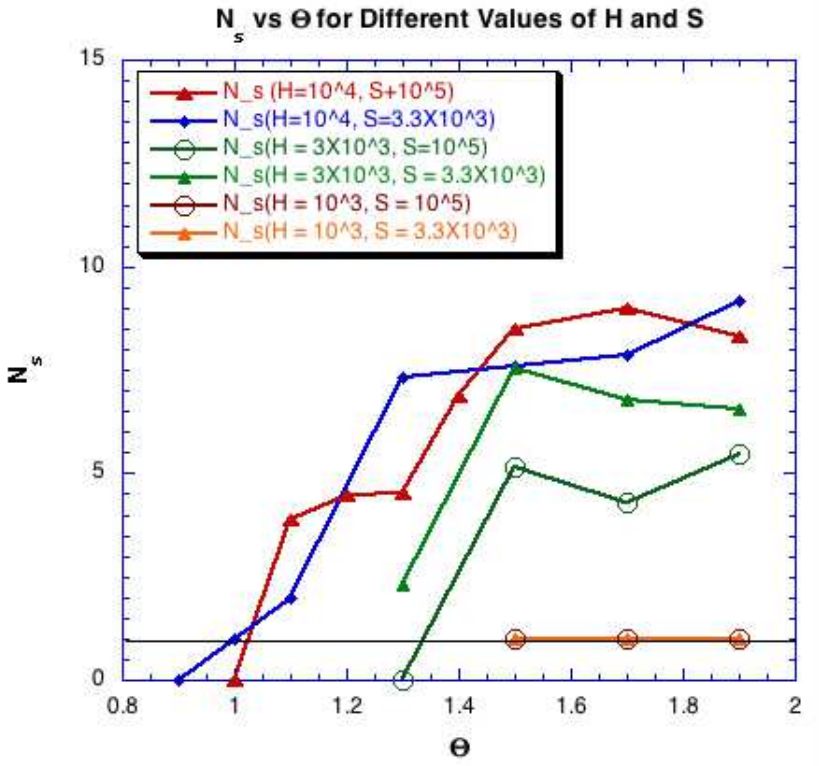

Figure 4: N_s, the number of $m = 1$ mode present in the time asymptotic state, as a function of Θ_0, with $R/a = 4$, for different values of H and S. The cases $H = 10^3$ with $S = 3.3 \times 10^3$ and $S = 10^5$ are single helicity for all Θ_0 (lower right). The case $H = 10^4$ and $S = 3.3 \times 10^3$ is single helicity when $\Theta_0 = 1$. All other states are either multi-helicity ($N_s > 1$) or stable ($N_s = 0$).

There is a trend toward deeper reversal with increasing H, but it does not seem strong.

Experimentally, single helicity states seem to favor shallow reversal, large S, and high current[9, 10, 11]. The results plotted in Figures 4 and 5 allow us to determine N_s as a function of F from the force-free visco-resistive model. These data are plotted in Figure 6. Single helicity states only occur when $H = 10^3$, independent of S. There is no indication of the appearance of single helicity at shallow reversal.

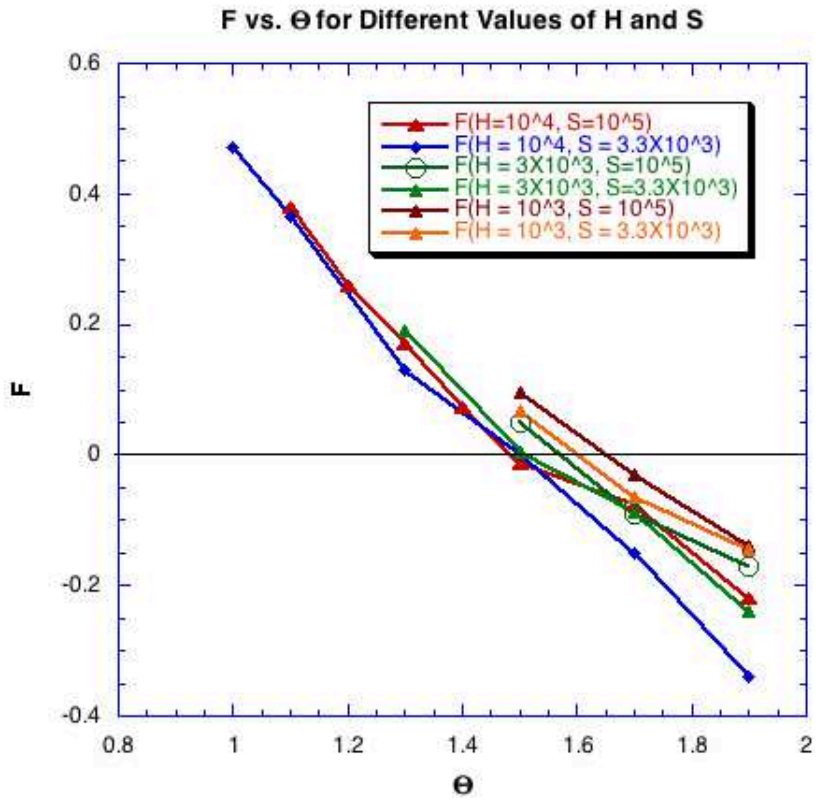

Figure 5: The reversal parameter F as a function of the pinch parameter Θ_0 for different values of H and S. For these parameters, reversal occurs in the range $1.45 < \Theta_0 < 1.7$. There is a trend toward deeper reversal with increasing H, but it does not seem strong.

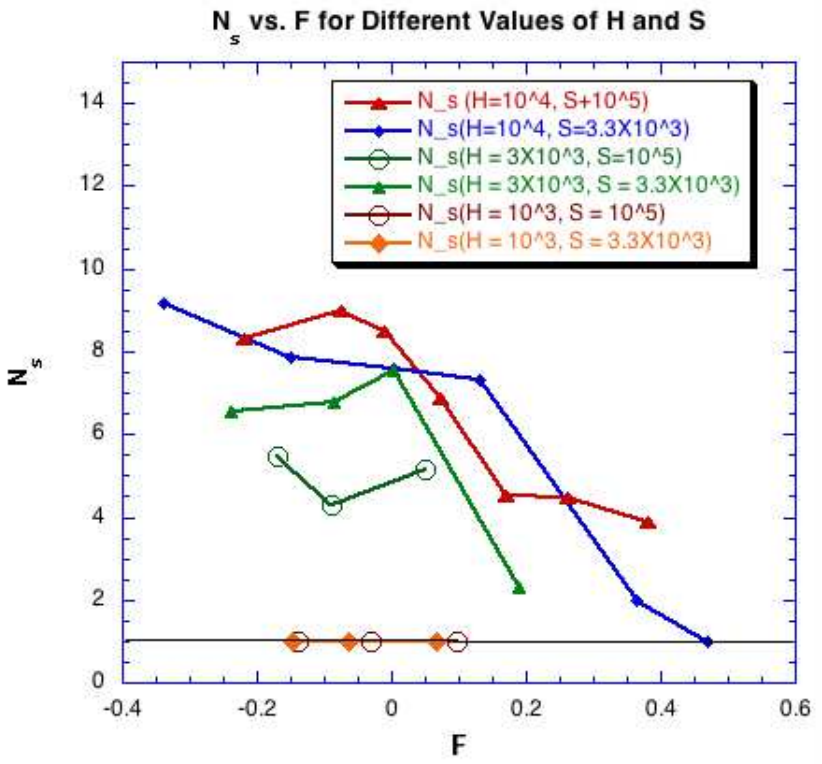

Figure 6: N_s as a function of the reversal parameter F for different values of H and S. For these parameters, single helicity only occurs when $H = 10^3$, independent of S. There is no indiction of the appearance of single helicity at shallow reversal.

3 Summary

We have examined the appearance of single-helicity (SH) and multi-helicity (MH) states as a function of H, S (or equivalently P_M), and Θ_0 with $R/a = 4$ using the force-free visco-resistive MHD model as solved with the DEBS code. We have used the time average of the parameter N_s, Equation (9), as a proxy for these states; $N_s = 1$ corresponds to SH, and $N_s > 1$ to MH. We have labeled a stable state by assigning the value $N_s = 0$. We have found that, for $\Theta_0 = 1.9$, a transition from SH to MH states occurs when $H > 2000 - 3000$, independent of S; see Figure 3. This is in substantial agreement with the results of Refs. [4] and [5]. Further, the marginal stability point is found to depend only on H (stable for $H < 200$), independent of S, again in agreement with the predictions of Ref. [4].

We have also examined the appearance of SH and MH states as a function of Θ_0 for different values of H and S; see Figure 4. We have found that, while there is clearly a trend toward fewer $m = 1$ modes with decreasing Θ_0, the presence of single helicity is most strongly influenced by H. The marginal stability point ($N_s = 0$) is approximately constant for a given value of H, independent of S, and consistent with Ref. [4], although the results are not as clear as in Figure 3.

Since the field reversal parameter F is determined by the remaining parameters, we can determined F as a function of Θ_0 for the cases considered; see Figure 5. For these parameters, reversal occurs in the range $1.45 < \Theta_0 < 1.7$. There is a trend toward deeper reversal with increasing H, but it does not seem strong.

Since the dependence of F on Θ_0 is single valued, we can also determine N_s, Equation (9), as a function of F; see Figure 6. Again, the appearance of SH states is seen to depend only on H, independent of S. There is no indication of the appearance of single helicity with shallow reversal.

Taken together, these results indicate that, *within the force-free visco-resistive MHD model, the transition from MH to SH states depends primarily on H, and is largely independent of S and Θ_0*. There is no dependence on the degree of field reversal.

These results contradict the experimental trends, in which SH states occur preferentially at shallow reversal, high current, and large S[9, 10, 11]. In terms of experimental parameters, and assuming Spitzer resistivity, the Lundquist number scales as $S \sim IT_e^{3/2}/(\Theta_0\sqrt{n})$, where I is the current, T_e is the electron temperature, and n is the number density. Thus, S increases with larger current, lower density, and smaller Θ (i.e., shallow reversal). In order for the experimental trends (increasing appearance of SH with increasing S) to be consistent with the force-free visco-resistive MHD results (increasing appearance of SH with decreasing H, independent of S), H must scale with the experimental parameters in the *opposite* direction of S.

The Hartmann number H depends equally on the viscosity and the resistivity,

and very little is known about the local viscosity in fusion plasmas. However, we can consider two idealized cases: the classical parallel and perpendicular viscosities from Braginskii. These are $\nu_\parallel \sim T/\nu_c$ and $\nu_\perp \sim T\nu_c/\Omega^2$, where $\nu_c \sim n/T^{3/2}$ is the collision frequency and $\Omega \sim B$ is the gyro-frequency. Then the corresponding viscous diffusion times scale like $\tau_{\nu\parallel} \sim nT^{-5/2}$ and $\tau_{\nu\perp} \sim B^2T^{1/2}/n$. The resistive diffusion time scales like $\tau_R \sim T^{3/2}$, and the Alfvén time scales like $\tau_A \sim B/\sqrt{n}$. Then using $B \sim I/\Theta_0$, the Hartmann numbers $H = \sqrt{\tau_\nu \tau_R}/\tau_A$ corresponding to the two cases scale like $H_\parallel \sim n\Theta_0/(T^{1/2}I)$ and $H_\perp \sim T^{5/4}$. The Hartmann number corresponding to the *parallel* viscosity scales in the required direction, i.e., it *decreases* with increasing current and temperature, and with decreasing density and Θ_0; it is consistent with the experimental trends. The perpendicular Hartmann number depends only on the temperature, and is independent of the current, density, and Θ_0.

It is often argued that, since MHD deals primarily with flows *perpendicular* to the magnetic field, the viscosity should be based on $\nu_\perp$. Nonetheless, the foregoing simple arguments show that, for the 'collisional" viscosity, the parallel viscosity results in a scaling that is at least consistent with experimental trends, while the perpendicular viscosity does not. This is also consistent with Ref. [4], where it was reported that estimates of the order of magnitude of the MHD stability threshold in (H, Θ_0) space based on JET data were much better described by the parallel viscosity than by the perpendicular viscosity; using the latter gave results that were in error by six orders of magnitude. Of course, it is probable that the viscosity (and even the form of the viscous stress tensor) is "anomalous", arising for example from turbulence or magnetic fluctuations. As stated in Ref. [4], "The larger question of justifying a convincing and manageable approximation of the viscous stress tensor for a hot plasma in a dc magnetic field has come to seem to us as perhaps the pivotal problem in deriving a workable theory ..." of MHD activity in fusion plasmas.

Other sources of uncertainty are boundary conditions, density and temperature variation (finite-β effects), plasma rotation, toroidal geometry, or perhaps something completely outside the visco-resistive MHD model.

References

[1] S. Ortolani and D. D. Schnack, *Magnetohydrodynamics of Plasma Relaxation*, World Scientific, Singapore, 1993.

[2] D. D. Schnack, D. C. Barnes, Z. Mikić, D. S. Harned, and E. J. Caramana, J. Comp. Phys. **70**, 330 (1987).

[3] S. Cappello and D. Biskamp, Nucl. Fusion **36**, 571 (1996).

[4] D. Montgomery, Plasma Phys. Cont. Fusion **34**, 1157 (1992).

[5] S. Cappello and D. F. Escande, Phys. Rev. Lett. **85**, 3838 (2000).

[6] S. Cappello and R. Paccagnella, Phys Fluid B **4**, 611 (1992).

[7] J. B. Taylor, Phys. Rev. Lett. **33**, 139 (1974).

[8] Y. L. Ho, D. D. Schnack, P. Nordlund, S. Mazur, H.-E. Satherblom, J. Scheffel and J. R. Drake, Phys. Plasmas **2**, 3407 (1995).

[9] Y. Hirano, R. Paccagnella, H. Koguchi, L. Frassinetti, H. Sakakita and Y. Yagi, Phys. Plasmas **11**, 112501 (2005).

[10] P. Martin, L. Apolloni, M. E. Puiatti, *et al.*, Nucl. Fusion **49**, 104019 (2009).

[11] B. E. Chapman, F. Auriemma, W. F. Bergerson, *et. al.*, paper EX/P6-01, IAEA Fusion Energy Conference, San Diego (2012).